fractal and fractional

MDPI

Article

On the Convergence Rate of the Caputo Fractional Difference Logistic Map of Nilpotent Matrices

Rasa Smidtaite [1], Algirdas Kazlauskas [1], Mark Edelman [2,3] and Minvydas Ragulskis [1,*]

[1] Research Group for Nonlinear Systems, Kaunas University of Technology, Studentu 50-146, 51368 Kaunas, Lithuania; rasa.smidtaite@ktu.lt (R.S.); algirdas.kazlauskas@ktu.edu (A.K.)
[2] Stern College for Women, Yeshiva University, 45 Lexington Ave., New York, NY 10016, USA; edelman@cims.nyu.edu
[3] Courant Institute of Mathematical Sciences, New York University, 251 Mercer Street, New York, NY 10012, USA
* Correspondence: minvydas.ragulskis@ktu.lt; Tel.: +370-698-22456

Abstract

The convergence rate of the Caputo fractional difference logistic map of nilpotent matrices is investigated in this paper. The divergence rate of the auxiliary parameters governing the dynamics of nilpotents is exponential and is multiple to the Lyapunov exponent of the scalar non-fractional map. However, the convergence of the Caputo fractional difference logistic map of nilpotent matrices to a stable fixed point is governed by the interplay between the convergence rate of the scalar fractional map (the power law rate) and the exponential convergence induced by the nilpotent matrices. It is demonstrated that convergence is determined by the competition between the power law and exponential mechanisms, a feature not captured by scalar fractional maps, with higher-order auxiliary parameters diverging exponentially at increasingly higher rates. This paper provides insight into the complex dynamics of fractional maps of nilpotent matrices.

Keywords: fractional difference logistic map; nilpotent matrix; convergence rate; Lyapunov exponent

1. Introduction

A logistic map was introduced (but it was not called the logistic map at the time of its introduction) in Edward Lorenz's paper [1] (see Equation (3) in that paper). This map acquired its popularity after the 1976 Nature publication by Sir Robert M. May [2] in which the author described the logistic map's transition to chaos through the period-doubling cascade of bifurcations. The meaning of the term cascade of bifurcations is that at a certain value of the map's parameter a, a stable period l point becomes unstable, and a stable period $2l$ point is born. When a continues its monotonic evolution, this process continues until the onset of chaos. This universal self-similar behavior is typical for almost all nonlinear maps, and its universality is characterized by the existence of the Feigenbaum function and constants (see, e.g., paper [3] and a book, [4]). The main applications considered by May were biological (even the variable used in the text was treated as "the population") as well as from the social sciences and economics. As it is related to the topic of the present publication, we must note that the convergence of the logistic map's trajectories to periodic points is exponential, except for the countable set of bifurcation points (see, e.g., the Lyapunov exponent graph [5,6]).

Academic Editor: Ivanka Stamova

Received: 4 December 2025
Revised: 1 January 2026
Accepted: 6 January 2026
Published: 8 January 2026

As we mentioned, the main applications of the logistic map are for biological [7–9], social [10–12], and economic [13–15] systems. But all these systems possess memory, which in most cases is asymptotically power law memory (see, e.g., citations in [16] for examples of power law memory in biology and [17] for economic applications). Equations/maps with asymptotically power law memory also play an important role in control theory (see, e.g., [18–20]) and signal/image processing and encryption (see, e.g., [21–23]). Maps with power law memory and arbitrary time steps (called fractional maps) may be introduced directly, as was performed in [24]. When the maps' time steps tend to zero, these maps converge to the corresponding fractional differential equations. A wide class of maps with asymptotically power law memory, which includes the majority of maps derived from fractional differential equations or as solutions of fractional difference equations, called generalized fractional maps, was introduced in [25]; most recent advances are reported in [26]. Generalized fractional maps are Volterra difference equations of the convolution type with power law-like kernels. When the kernels are falling factorials, generalized fractional maps become fractional difference maps, which are the most popular maps used in many applications. The present paper utilizes the fractional difference logistic map introduced in [27].

Fractional and fractional difference maps possess some common properties that differ from the properties of regular maps. Here, we will mention those properties that are relevant to the present publication concerning the fractional difference logistic map.

- The fractional difference logistic map has no periodic points except for the fixed points, but it has asymptotically periodic points [28–30].
- The equations defining the asymptotically periodic points of the fractional difference logistic map were derived in [25]; the infinite sums that define the coefficients of these equations were calculated in [31]. The equations defining asymptotic bifurcation points were derived in [32].
- The finite time evolution of the fractional difference logistic map is characterized by [33] as a cascade of bifurcation-type trajectories and an inverse cascade of bifurcation-type trajectories. In a cascade of bifurcation-type trajectories, cascades of bifurcations are not the result of changes in map parameters, but they occur on single trajectories during the trajectories' time evolution (iterations). In the fractional difference logistic map, an asymptotically stable period $2^i l$ or asymptotically chaotic trajectories with the initial conditions near zero start converging to the unstable period's l trajectory, but then bifurcate and start converging to the period's $2l$ trajectory, and so on, until, after i consecutive bifurcations, they converge to the asymptotically stable trajectory or become chaotic. The fractional difference logistic map's asymptotically stable period's p trajectories with the initial conditions near one may initially converge to period $p \times 2^i$ trajectories, and after i consecutive mergers (inverse bifurcations), converge to the stable trajectories (see examples in [16]).
- Numerical simulations show that, in fractional and fractional difference maps, convergence to the asymptotically stable periodic points follows the power law. In the case of convergence to the asymptotically stable fixed points of fractional difference maps, the power law convergence was strictly proven in [34]. In a cascade of bifurcation-type trajectories, as is shown in [16], the initial convergence to an unstable fixed point prior to a bifurcation also follows the same power law.

As is shown in [35], the complexity of a discrete system can be increased not only by extending its spatial dimension (by introducing coupled map lattices [36–38]), but also by replacing the scalar iterative variable by the square matrix of iterative variables. Indeed, unexpected phenomena, such as finite-time and explosive divergence, can be observed

in the iterative logistic map of second-order matrices if and only if the matrix of initial conditions has a recurrent eigenvalue (and is not a scalar matrix) [35].

Formal algebraic techniques are employed to define the effect of explosive divergence in generalized maps of iterative matrices in [39]. The necessary and sufficient conditions for the generation of complex spatiotemporal patterns in 2D coupled iterative maps of nth order matrices are derived and used in multiple-image hiding schemes in [40]. The Caputo fractional difference logistic map of matrices enables the observation of the original isolated waves of temporary divergence, located far away from the initial conditions [41].

In all real-world applications, the convergence rate plays a crucial role [42–44]. It is a critical factor in the chaos control and synchronization of dynamical systems, directly impacting system performance and stability [45–47]. Fast convergence ensures that the system quickly reaches the desired synchronized state, minimizing the effects of disturbances, delays, and uncertainties [48–50]. Moreover, a higher convergence rate improves efficiency by reducing energy consumption and communication overhead, which is essential for real-world applications such as power grids [51–53], multi-agent systems [54–56], and networked control systems [57–59]. Due to the fact that in many cases fractional-order models describe real systems in interdisciplinary fields more elegantly than integer-order models, the analysis of fractional systems has attracted significant attention in physics [60–62], biology [63–65], engineering [66–68], and economics [69–72]. Recent advancements in the convergence control of fractional-order systems are reported in [73–75]. It is known that, unlike in the case of the integer-order derivative, fractional systems have only asymptotically periodic solutions, except at fixed points [30,76]. The power law convergence for the fixed points, the period-two points, and the divergence are investigated numerically and analytically in the fractional standard map with the Riemann–Liouville fractional derivative of order ν ($1 < \nu \leq 2$) [33]. The rate of convergence for the Caputo logistic map is analyzed in [27]. The numerical and semi-analytical investigation for the Caputo fractional difference logistic map with the fractional order $\nu > 0$ is provided [16,27]. The stability conditions are derived, and the decay rate for the fractional Caputo difference map of order $0 < \nu < 1$ is shown to be $k^{-\nu}$, where k denotes the number of iterations [77].

The main objective of this paper is to investigate the convergence rates in the Caputo fractional difference logistic map of nth order nilpotent matrices by emphasizing the competitive behavior between the power law and the exponential convergence rates obeying map components. This paper is structured as follows. The fundamental properties of the iterative maps of matrices are discussed in Section 2. The Caputo fractional difference logistic map of nth order nilpotent matrices is presented in Section 3. The divergence rate of the fractional difference logistic map of nilpotent matrices is investigated analytically and computationally in Section 4. The convergence of the fractional difference logistic map of nilpotent matrices is explored in Section 5. The discussion and concluding remarks are given in the last section.

2. Preliminaries

2.1. The Logistic Map of Matrices

The classical logistic map reads in [2] as follows:

$$x^{(k+1)} = a\, x^{(k)} \left(1 - x^{(k)}\right), \tag{1}$$

where k is the iteration number ($k = 0, 1, 2, \ldots$), a is the parameter of the logistic map $a \in \mathbb{R}$ (bounded on the interval $0 \leq a \leq 4$), and $x^{(0)}$ is the initial condition (bounded on the interval $0 \leq x^{(0)} \leq 1$).

The scalar variable $x^{(k)}$ in (1) can be replaced by a square matrix $\mathbf{X}^{(k)}$ to obtain a logistic map of matrices [35,39]:

$$\mathbf{X}^{(k+1)} = a\,\mathbf{X}^{(k)}\left(\mathbf{I} - \mathbf{X}^{(k)}\right), \tag{2}$$

where $\mathbf{X}^{(k)} \in \mathbb{R}^{n\times n}$ (n is the order of square matrix $\mathbf{X}^{(k)}$) and $\mathbf{I}$ denotes the identity matrix. The dynamics of the logistic map of matrices depends on the form of the initial condition matrix $\mathbf{X}^{(0)}$, the three possible forms being an idempotent, a scalar, or a nilpotent matrix [35,39]. It is demonstrated in [41] that idempotent and scalar matrices do not change the complexity of the scalar Caputo fractional difference logistic map of matrices. However, nilpotent matrices induce such effects as finite-time divergence, intermittent bursting, and explosive divergence in iterative maps of matrices [41]. Therefore, all further analysis is focused only on the fractional difference logistic map of nilpotent matrices.

2.2. The Logistic Map of Nilpotent Matrices

Let us assume that all eigenvalues $\lambda_j^{(0)}$ ($j = 1, 2, \ldots, n$) of the matrix of initial conditions $\mathbf{X}^{(0)}$ are identical:

$$\lambda_1^{(0)} = \lambda_2^{(0)} = \ldots = \lambda_n^{(0)} := \lambda_0^{(0)}. \tag{3}$$

Then, $\mathbf{X}^{(0)}$ in a single Jordan block reads as follows [39]:

$$\mathbf{X}^{(0)} = \lambda_0^{(0)}\mathbf{I} + \mu_1^{(0)}\mathbf{N}_1 + \mu_2^{(0)}\mathbf{N}_2 + \ldots + \mu_{n-1}^{(0)}\mathbf{N}_{n-1}, \tag{4}$$

where $\mu_1^{(0)}$, $\mu_2^{(0)}$, …, $\mu_{n-1}^{(0)} \in \mathbb{R}$ ($\mu_1^{(0)} \neq 0$) and $\mathbf{N}_j$ ($j = 1, 2, \ldots, n-1$) denotes a nilpotent $\mathbf{N}_j = \mathbf{T}\mathbf{L}^{[j]}\mathbf{T}^{-1}$, $\mathbf{T} \in \mathbb{R}^{n\times n}$, $\det\mathbf{T} \neq 0$. The canonical nilpotent $\mathbf{L}^{[j]}$ represents a matrix of order $n \times n$ with jth superdiagonal of ones and all other entries equal to zero.

Nilpotents $\mathbf{N}_j$ ($j = 1, 2, \ldots, n-1$) satisfy the following equalities [39]:

$$\det\mathbf{N}_j = 0, \quad \mathbf{N}_i \cdot \mathbf{N}_j = \begin{cases} \mathbf{N}_{i+j}, & i + j \leq n-1; \\ \mathbf{\Theta}, & i + j > n-1. \end{cases} \tag{5}$$

Example 1. *The matrix of initial conditions* $\mathbf{X}^{(0)} = \begin{bmatrix} 1&2&3&4&5&6 \\ 0&1&2&3&4&5 \\ 0&0&1&2&3&4 \\ 0&0&0&1&2&3 \\ 0&0&0&0&1&2 \\ 0&0&0&0&0&1 \end{bmatrix}$ *can be decomposed into the canonical form comprising five different nilpotents:*

$$\mathbf{X}^{(0)} = \lambda_0^{(0)}\mathbf{I} + \mu_1^{(0)}\mathbf{N}_1 + \mu_2^{(0)}\mathbf{N}_2 + \mu_3^{(0)}\mathbf{N}_3 + \mu_4^{(0)}\mathbf{N}_4 + \mu_5^{(0)}\mathbf{N}_5, \tag{6}$$

where $\lambda_0^{(0)} = 1$, $\mu_1^{(0)} = 2$, $\mu_2^{(0)} = 3$, $\mu_3^{(0)} = 4$, $\mu_4^{(0)} = 5$, $\mu_5^{(0)} = 6$, *and*

$$\begin{aligned} &\mathbf{N}_1 = \mathbf{L}^{[1]} = \begin{bmatrix} 0&1&0&0&0&0 \\ 0&0&1&0&0&0 \\ 0&0&0&1&0&0 \\ 0&0&0&0&1&0 \\ 0&0&0&0&0&1 \\ 0&0&0&0&0&0 \end{bmatrix}, \quad \mathbf{N}_2 = \mathbf{L}^{[2]} = \begin{bmatrix} 0&0&1&0&0&0 \\ 0&0&0&1&0&0 \\ 0&0&0&0&1&0 \\ 0&0&0&0&0&1 \\ 0&0&0&0&0&0 \\ 0&0&0&0&0&0 \end{bmatrix}, \quad \mathbf{N}_3 = \mathbf{L}^{[3]} = \begin{bmatrix} 0&0&0&1&0&0 \\ 0&0&0&0&1&0 \\ 0&0&0&0&0&1 \\ 0&0&0&0&0&0 \\ 0&0&0&0&0&0 \\ 0&0&0&0&0&0 \end{bmatrix}, \\ &\mathbf{N}_4 = \mathbf{L}^{[4]} = \begin{bmatrix} 0&0&0&0&1&0 \\ 0&0&0&0&0&1 \\ 0&0&0&0&0&0 \\ 0&0&0&0&0&0 \\ 0&0&0&0&0&0 \\ 0&0&0&0&0&0 \end{bmatrix}, \quad \mathbf{N}_5 = \mathbf{L}^{[5]} = \begin{bmatrix} 0&0&0&0&0&1 \\ 0&0&0&0&0&0 \\ 0&0&0&0&0&0 \\ 0&0&0&0&0&0 \\ 0&0&0&0&0&0 \\ 0&0&0&0&0&0 \end{bmatrix}. \end{aligned} \tag{7}$$

Definition 1. *The matrix of initial conditions* $\mathbf{X}^{(0)}$ *expressible in the form (4) is defined as the nilpotent matrix.*

As shown in [39], the logistic map of matrices (2) with a nilpotent matrix of initial conditions preserves the same nilpotents $\mathbf{N}_j$ $(j = 1, 2, \ldots, n-1)$ for each consecutive iteration:

$$\mathbf{X}^{(k+1)} = \lambda_0^{(k+1)}\mathbf{I} + \mu_1^{(k+1)}\mathbf{N}_1 + \mu_2^{(k+1)}\mathbf{N}_2 + \ldots + \mu_{n-1}^{(k+1)}\mathbf{N}_{n-1}, \quad k = 0, 1, 2, \ldots, \tag{8}$$

where

$$\begin{cases} \lambda_0^{(k+1)} = a\lambda_0^{(k)}\left(1 - \lambda_0^{(k)}\right); \\ \mu_1^{(k+1)} = a\mu_1^{(k)}\left(1 - 2\lambda_0^{(k)}\right); \\ \mu_2^{(k+1)} = a\mu_2^{(k)}\left(1 - 2\lambda_0^{(k)}\right) - a\left(\mu_1^{(k)}\right)^2; \\ \ldots \\ \mu_{n-1}^{(k+1)} = a\mu_{n-1}^{(k)}\left(1 - 2\lambda_0^{(k)}\right) - a\sum\limits_{s=1}^{n-2}\mu_s^{(k)}\mu_{n-1-s}^{(k)}; \end{cases} \tag{9}$$

and $\mu_s^{(0)} \neq 0; s = 1, 2, \ldots, n-1$.

Definition 2. *The system of intertwined iterative maps* (9) *is defined as the logistic map of the nth order nilpotent matrices.*

2.3. The Divergence Rate of the Logistic Map of Nilpotent Matrices

The logistic map of nilpotent matrices can become explosive even if a recurrent eigenvalue remains bounded (Equation (1)). The logistic map of matrices becomes explosive if the Lyapunov exponent of the scalar logistic map is positive and the matrix of initial conditions is a nilpotent matrix [39]. It is demonstrated in [39] that the divergence rate of the auxiliary parameters $\mu_s^{(k)}; s = 1, 2, \ldots, n-1$ is exponential when the dynamics of $\lambda_0^{(k)}$ is chaotic and the Lyapunov exponent L of this scalar sequence is positive.

2.4. The Fractional Difference Logistic Map

The fractional difference logistic map is described by the following recurrence equation [27,41]:

$$x^{(k)} = x^{(0)} + \sum_{j=1}^{k} G_{j-1}(a\, x^{(k-j)}\left(1 - x^{(k-j)}\right) - x^{(k-j)}), \tag{10}$$

where $k = 1, 2, \ldots$ and the governing equation for G_j is

$$G_j = \left(1 - \frac{1-\nu}{j}\right)G_{j-1}, \quad G_0 = 1, \tag{11}$$

where the parameter ν describes the order of the fractional difference from the interval $0 < \nu \leq 1$ [27,78].

Note that Equation (10) reduces to the classical logistic map (1) when the fractional order ν is set to 1.

2.5. The Fractional Difference Logistic Map of Matrices

The scalar variable $x^{(k)}$ in Equation (10) can be replaced by a square matrix $\mathbf{X}^{(k)}$ to obtain a fractional logistic map of the matrices [41]:

$$\mathbf{X}^{(k)} = \mathbf{X}^{(0)} + \sum_{j=1}^{k} G_{j-1}\left(a\mathbf{X}^{(k-j)}\left(\mathbf{I} - \mathbf{X}^{(k-j)}\right) - \mathbf{X}^{(k-j)}\right), \tag{12}$$

where G_j is defined by (11) and $\mathbf{X}^{(0)} \in \mathbb{R}^{n\times n}$ is the matrix of the initial conditions.

2.6. The Motivation of This Study

As already mentioned in the Introduction, the convergence rate plays a critical role in many real-world applications. It has already been discussed that the divergence rate of the logistic map of nilpotent matrices is exponential, but the fractional difference scalar logistic map converges to fixed points according to the power law. The behavior of the fractional difference logistic map of nilpotent matrices is completely unclear in that sense, and thus constitutes the main objective of this paper.

3. The Fractional Difference Logistic Map of Nilpotent Matrices

The complexity of an iterative model can be increased not only by extending the number of coupled nodes in the spatial domain, but also by increasing the complexity of each individual node [39]. One effective way to enhance nodal complexity is to replace a scalar variable with a matrix-valued variable in an iterative map [35]. On the other hand, fractional difference iterative maps provide a powerful framework for studying systems in which memory effects play a significant role in their evolution [27,79,80]. Consequently, incorporating matrix-valued variables into fractional difference iterative maps represents a natural and timely extension that opens new avenues for the investigation of complex fractional systems.

Let us assume that the matrix of initial conditions $\mathbf{X}^{(0)}$ is a nth order nilpotent matrix (Equation (4)). Then the fractional difference logistic map of matrices (Equation (12)) reads

$$\begin{aligned}
\mathbf{X}^{(k)} &= \lambda_0^{(0)}\mathbf{I} + \mu_1^{(0)}\mathbf{N}_1 + \mu_2^{(0)}\mathbf{N}_2 + \ldots + \mu_{n-1}^{(0)}\mathbf{N}_{n-1} \\
&\quad + \sum_{j=1}^{k} G_{j-1}\Big(a\Big(\lambda_0^{(k-j)}\mathbf{I} + \mu_1^{(k-j)}\mathbf{N}_1 + \mu_2^{(k-j)}\mathbf{N}_2 + \ldots + \mu_{n-1}^{(k-j)}\mathbf{N}_{n-1}\Big) \\
&\qquad\qquad \times \Big(\mathbf{I} - \Big(\lambda_0^{(k-j)}\mathbf{I} + \mu_1^{(k-j)}\mathbf{N}_1 + \mu_2^{(k-j)}\mathbf{N}_2 + \ldots + \mu_{n-1}^{(k-j)}\mathbf{N}_{n-1}\Big)\Big) \\
&\qquad\qquad - \Big(\lambda_0^{(k-j)}\mathbf{I} + \mu_1^{(k-j)}\mathbf{N}_1 + \mu_2^{(k-j)}\mathbf{N}_2 + \ldots + \mu_{n-1}^{(k-j)}\mathbf{N}_{n-1}\Big)\Big) \\
&= \left(\lambda_0^{(0)} + \sum_{j=1}^{k} G_{j-1}\Big(a\lambda_0^{(k-j)}\Big(1-\lambda_0^{(k-j)}\Big) - \lambda_0^{(k-j)}\Big)\right)\mathbf{I} \\
&\quad + \left(\mu_1^{(0)} + \sum_{j=1}^{k} G_{j-1}\Big(a\mu_1^{(k-j)}\Big(1-2\lambda_0^{(k-j)}\Big) - \mu_1^{(k-j)}\Big)\right)\mathbf{N}_1 \\
&\quad + \left(\mu_2^{(0)} + \sum_{j=1}^{k} G_{j-1}\Big(a\mu_2^{(k-j)}\Big(1-2\lambda_0^{(k-j)}\Big) - a\Big(\mu_1^{(k-j)}\Big)^2 - \mu_2^{(k-j)}\Big)\right)\mathbf{N}_2 + \ldots \\
&\quad + \left(\mu_{n-1}^{(0)} + \sum_{j=1}^{k} G_{j-1}\left(a\mu_{n-1}^{(k-j)}\Big(1-2\lambda_0^{(k-j)}\Big) - a\sum_{s=1}^{n-2}\mu_s^{(k-j)}\mu_{n-1-s}^{(k-j)} - \mu_{n-1}^{(k-j)}\right)\right)\mathbf{N}_{n-1},
\end{aligned} \tag{13}$$

since the multiplication of two nilpotents is obtained by applying Equation (5). Therefore, the fractional difference logistic map of nilpotent matrices splits into n scalar intertwined maps. In other words, the dynamics of the fractional difference logistic map of nilpotent matrices is governed by a single scalar fractional difference logistic map of the recurrent eigenvalue $\lambda_0^{(k)}$, and $n-1$ scalar intertwined maps of the auxiliary parameters $\mu_1^{(k)}$, $\mu_2^{(k)}$, $\ldots$, $\mu_{n-1}^{(k)}$:

$$\begin{cases} \lambda_0^{(k)} = \lambda_0^{(0)} + \sum\limits_{j=1}^{k} G_{j-1}\left(a\lambda_0^{(k-j)}\left(1-\lambda_0^{(k-j)}\right) - \lambda_0^{(k-j)}\right); \\ \mu_1^{(k)} = \mu_1^{(0)} + \sum\limits_{j=1}^{k} G_{j-1}\left(a\mu_1^{(k-j)}\left(1-2\lambda_0^{(k-j)}\right) - \mu_1^{(k-j)}\right); \\ \mu_2^{(k)} = \mu_2^{(0)} + \sum\limits_{j=1}^{k} G_{j-1}\left(a\mu_2^{(k-j)}\left(1-2\lambda_0^{(k-j)}\right) - a\left(\mu_1^{(k-j)}\right)^2 - \mu_2^{(k-j)}\right); \\ \ldots \\ \mu_{n-1}^{(k)} = \mu_{n-1}^{(0)} + \sum\limits_{j=1}^{k} G_{j-1}\left(a\mu_{n-1}^{(k-j)}\left(1-2\lambda_0^{(k-j)}\right) - a\sum\limits_{s=1}^{n-2}\mu_s^{(k-j)}\mu_{n-1-s}^{(k-j)} - \mu_{n-1}^{(k-j)}\right); \end{cases} \tag{14}$$

where $k = 1, 2, \ldots; \mu_s^{(0)} \neq 0; s = 1, 2, \ldots, n-1$ and G_j is given by Equation (11).

Definition 3. *The system of intertwined iterative maps (Equation (14)) is defined as the fractional difference logistic map of the nth order nilpotent matrices.*

Example 2. *Let us consider the 6th order nilpotent matrix as a matrix of initial conditions. Then the iterated map of the highest order auxiliary parameter in Equation (14) reads*

$$\mu_5^{(k)} = \mu_5^{(0)} + \sum_{j=1}^{k} G_{j-1}\left(a\,\mu_5^{(k-j)}\left(1-2\lambda_0^{(k-j)}\right) - 2a\mu_1^{(k-j)}\mu_4^{(k-j)} - 2a\mu_2^{(k-j)}\mu_3^{(k-j)} - \mu_5^{(k-j)}\right). \tag{15}$$

Corollary 1. *The fractional difference logistic map of nilpotent matrices (14) converges to the logistic map of nilpotent matrices (9) when the fractional order ν is equal to integer value 1.*

Proof. Let us investigate the expression of $\lambda_0^{(k)}$ in the fractional difference logistic map of matrices (14) when the fractional order ν is set to 1:

$$\begin{aligned} \lambda_0^{(k)} &= \lambda_0^{(0)} + \sum_{j=1}^{k} G_{j-1}\left(a\lambda_0^{(k-j)}\left(1-\lambda_0^{(k-j)}\right) - \lambda_0^{(k-j)}\right) \\ &= \lambda_0^{(0)} + G_0\left(a\lambda_0^{(k-1)}\left(1-\lambda_0^{(k-1)}\right) - \lambda_0^{(k-1)}\right) + G_1\left(\underbrace{a\lambda_0^{(k-2)}\left(1-\lambda_0^{(k-2)}\right)}_{\lambda_0^{(k-1)}} - \lambda_0^{(k-2)}\right) + \ldots \\ &\quad + G_{k-2}\left(\underbrace{a\lambda_0^{(k-(k-1))}\left(1-\lambda_0^{(k-(k-1))}\right)}_{\lambda_0^{(2)}} - \lambda_0^{(k-(k-1))}\right) \\ &\quad + G_{k-1}\left(\underbrace{a\lambda_0^{(k-k)}\left(1-\lambda_0^{(k-k)}\right)}_{\lambda_0^{(1)}} - \lambda_0^{(k-k)}\right) \\ &= \lambda_0^{(0)} + a\lambda_0^{(k-1)}\left(1-\lambda_0^{(k-1)}\right) - \lambda_0^{(k-1)} + \lambda_0^{(k-1)} - \lambda_0^{(k-2)} + \lambda_0^{(k-2)} - \lambda_0^{(k-3)} + \ldots \\ &\quad + \lambda_0^{(1)} - \lambda_0^{(0)} = \\ &= a\lambda_0^{(k-1)}\left(1-\lambda_0^{(k-1)}\right), \end{aligned} \tag{16}$$

where $G_j = G_{j-1}$ $(j = 1, 2, \ldots, k; G_0 = 1)$ if $\nu = 1$ (see Equation (11)).

Now, let us consider the general expression of auxiliary parameter $\mu_{n-1}^{(k)}$ in Equation (14) when $\nu = 1$:

$$\begin{aligned}
\mu_{n-1}^{(k)} &= \mu_{n-1}^{(0)} + \sum_{j=1}^{k} G_{j-1}\left(a\mu_{n-1}^{(k-j)}\left(1-2\lambda_0^{(k-j)}\right) - a\sum_{s=1}^{n-2}\mu_s^{(k-j)}\mu_{n-1-s}^{(k-j)} - \mu_{n-1}^{(k-j)}\right) \\
&= \mu_{n-1}^{(0)} + G_0\left(a\mu_{n-1}^{(k-1)}\left(1-2\lambda_0^{(k-1)}\right) - a\sum_{s=1}^{n-2}\mu_s^{(k-1)}\mu_{n-1-s}^{(k-1)} - \mu_{n-1}^{(k-1)}\right) \\
&\quad + G_1\left(\underbrace{a\mu_{n-1}^{(k-2)}\left(1-2\lambda_0^{(k-2)}\right) - a\sum_{s=1}^{n-2}\mu_s^{(k-2)}\mu_{n-1-s}^{(k-2)}}_{\mu_{n-1}^{(k-1)}} - \mu_{n-1}^{(k-2)}\right) + \ldots \\
&\quad + G_{k-2}\left(\underbrace{a\mu_{n-1}^{(k-(k-1))}\left(1-2\lambda_0^{(k-(k-1))}\right) - a\sum_{s=1}^{n-2}\mu_s^{(k-(k-1))}\mu_{n-1-s}^{(k-(k-1))}}_{\mu_{n-1}^{(2)}} - \mu_{n-1}^{(k-(k-1))}\right) \\
&\quad + G_{k-1}\left(\underbrace{\mu_{n-1}^{(k-k)}\left(1-2\lambda_0^{(k-k)}\right) - a\sum_{s=1}^{n-2}\mu_s^{(k-k)}\mu_{n-1-s}^{(k-k)}}_{\mu_{n-1}^{(1)}} - \mu_{n-1}^{(k-k)}\right) \\
&= \mu_{n-1}^{(0)} + a\mu_{n-1}^{(k-1)}\left(1-2\lambda_0^{(k-1)}\right) - a\sum_{s=1}^{n-2}\mu_s^{(k-1)}\mu_{n-1-s}^{(k-1)} - \mu_{n-1}^{(k-1)} + \mu_{n-1}^{(k-1)} - \mu_{n-1}^{(k-2)} \\
&\quad + \mu_{n-1}^{(k-2)} - \mu_{n-1}^{(k-3)} + \ldots + \mu_{n-1}^{(1)} - \mu_{n-1}^{(0)} \\
&= a\mu_{n-1}^{(k-1)}\left(1-2\lambda_0^{(k-1)}\right) - a\sum_{s=1}^{n-2}\mu_s^{(k-1)}\mu_{n-1-s}^{(k-1)},
\end{aligned} \tag{17}$$

where $G_j = 1; j = 0, 1, 2, \ldots, k-1$.

The auxiliary parameters $\mu_1^{(k)}, \mu_2^{(k)}, \ldots, \mu_{n-2}^{(k)}$ in the fractional difference logistic map of matrices (14) become identical to the auxiliary parameters of the classical logistic map of matrices (9) at $\nu = 1$. □

4. The Divergence Rate of the Fractional Difference Logistic Map of Nilpotent Matrices

4.1. The Divergence Rate of μ_1

The fractional difference logistic map of nilpotent matrices (14) yields

$$\mu_1^{(1)} = \mu_1^{(0)} + G_0\left(a\mu_1^{(0)}\left(1-2\lambda_0^{(0)}\right) - \mu_1^{(0)}\right) = \mu_1^{(0)} f'\left(\lambda_0^{(0)}\right), \tag{18}$$

where $f'(x) = a(1-2x)$ is the derivative of the mapping function of the classical logistic map (1).

Then,

$$\begin{aligned}\mu_1^{(2)} &= \mu_1^{(0)} + \sum_{j=1}^{2} G_{j-1}\left(a\mu_1^{(2-j)}\left(1-2\lambda_0^{(2-j)}\right)-\mu_1^{(2-j)}\right)\\ &= \mu_1^{(0)} + G_0\left(a\mu_1^{(1)}\left(1-2\lambda_0^{(1)}\right)-\mu_1^{(1)}\right) + G_1\left(a\mu_1^{(0)}\left(1-2\lambda_0^{(0)}\right)-\mu_1^{(0)}\right)\\ &= \mu_1^{(0)} + \left(\mu_1^{(0)}f'\left(\lambda_0^{(0)}\right)f'\left(\lambda_0^{(1)}\right)-\mu_1^{(0)}f'\left(\lambda_0^{(0)}\right)\right) + \left(1-\frac{1-\nu}{1}\right)\left(\mu_1^{(0)}f'\left(\lambda_0^{(0)}\right)-\mu_1^{(0)}\right)\\ &= \mu_1^{(0)}f'\left(\lambda_0^{(0)}\right)f'\left(\lambda_0^{(1)}\right)-(1-\nu)\mu_1^{(0)}\left(f'\left(\lambda_0^{(0)}\right)-1\right).\end{aligned} \tag{19}$$

Further elementary iterative transformations yield

$$\mu_1^{(k)} = \mu_1^{(0)}\prod_{j=0}^{k-1} f'\left(\lambda_0^{(j)}\right) + \mathcal{O}(1-\nu). \tag{20}$$

Note that the Lyapunov exponent of the scalar classical logistic map $\lambda_0^{(k)} = f\left(\lambda_0^{(k-1)}\right)$ $(k = 1, 2, \ldots)$ reads [81]

$$L = \frac{1}{k}\sum_{j=0}^{k-1}\ln\left|f'\left(\lambda_0^{(j)}\right)\right|. \tag{21}$$

Therefore,

$$\lim_{\nu\to 1}\ln\left|\mu_1^{(k)}\right| = kL + \ln\left|\mu_1^{(0)}\right|. \tag{22}$$

In other words, when L is positive, the divergence rate of $\left|\mu_1^{(k)}\right|$ is exponential. Moreover, the slope of the linear equation that approximates the divergence of $\left|\mu_1^{(k)}\right|$ on the log–linear scale is equal to L. The order of the auxiliary parameter $\left|\mu_1^{(k)}\right|$ is equal to one. Consequently, the divergence rate of this auxiliary parameter is equal to $1L$.

4.2. The Divergence Rate of μ_2

Without loss of generality, let us consider the dynamics of $\mu_2^{(k+1)}$ governed by the non-fractional logistic map of nilpotent matrices (9): $\mu_2^{(k+1)} = a\mu_2^{(k)}\left(1-2\lambda_0^{(k)}\right) - a\left(\mu_1^{(k)}\right)^2$. Let us introduce two auxiliary maps:

$$\beta_2^{(k+1)} = a\beta_2^{(k)}\left(1-2\lambda_0^{(k)}\right); \quad \eta_2^{(k+1)} = a\left(\mu_1^{(k)}\right)^2; \quad k = 0, 1, 2, \ldots \tag{23}$$

Following (22), the divergence rate of $\left|\beta_2^{(k)}\right|$ is equal to the divergence rate of $\left|\mu_1^{(k)}\right|$ on the log–linear scale:

$$\ln\left|\beta_2^{(k)}\right| = kL + \ln\left|\beta_2^{(0)}\right|. \tag{24}$$

However, the divergence rate of $\left|\eta_2^{(k)}\right|$ is $2L$ on the log–linear scale:

$$\ln\left|\eta_2^{(k)}\right| = \ln a + 2\ln\left|\mu_1^{(k)}\right| = \ln a + 2\left(kL + \ln\left|\mu_1^{(0)}\right|\right). \tag{25}$$

Note that $\eta_2^{(k)} > 0$, but $\beta_2^{(k)} \in \mathbb{R}$; $k = 0, 1, 2, \ldots$. Let us assume that $\beta_2^{(k)} < 0$ for some k. Then, the growth of $\mu_2^{(k)}$ at $k \to \infty$ can be approximated by

$$\lim_{k\to\infty}\left|\mu_2^{(k)}\right| = \lim_{k\to\infty}\left(\left|\beta_2^{(k)}\right| + \eta_2^{(k)}\right) = L^k + (2L)^k. \tag{26}$$

Then,

$$\lim_{k\to\infty}\left|\frac{\mu_2^{(k+1)}}{\mu_2^{(k)}}\right| = \lim_{k\to\infty}\frac{L^{k+1}\left(1+2^{k+1}\right)}{L^k\left(1+2^k\right)} = 2L. \tag{27}$$

Therefore, the divergence rate of $\left|\mu_2^{(k)}\right|$ is exponential, and the slope of the linear equation that approximates the divergence is $2L$.

Next, let us assume that $\beta_2^{(k)} > 0$ for some k. Then,

$$\lim_{k\to\infty}\left|\mu_2^{(k)}\right| = \lim_{k\to\infty}\left|\beta_2^{(k)} - \eta_2^{(k)}\right| = (2L)^k - L^k. \tag{28}$$

Then,

$$\lim_{k\to\infty}\left|\frac{\mu_2^{(k+1)}}{\mu_2^{(k)}}\right| = \lim_{k\to\infty}\frac{L^{k+1}\left(2^{k+1}-1\right)}{L^k\left(2^k-1\right)} = 2L. \tag{29}$$

Thus, finally, for positive L, the divergence rate of $\left|\mu_2^{(k)}\right|$ is exponential, and the slope of the linear equation that approximates the divergence is $2L$. The auxiliary parameter $\left|\mu_2^{(k)}\right|$ is of order two. Therefore, the divergence rate of this auxiliary parameter is equal to $2L$.

4.3. The Divergence Rate of μ_{n-1}

Let us introduce the following auxiliary maps:

$$\beta_3^{(k+1)} = a\beta_3^{(k)}\left(1-2\lambda_0^{(k)}\right); \quad \eta_{1,2}^{(k+1)} = a\mu_1^{(k)}\mu_2^{(k)}; \quad \eta_{2,1}^{(k+1)} = a\mu_2^{(k)}\mu_1^{(k)}; \quad k = 0,1,2,\ldots \tag{30}$$

The divergence rate of $\ln\left|\beta_3^{(k)}\right|$ is equal to L. However,

$$\lim_{k\to\infty}\frac{1}{k}\ln\left|\eta_{1,2}^{(k)}\right| = \lim_{k\to\infty}\frac{1}{k}\ln\left|\eta_{2,1}^{(k)}\right| = L + 2L = 3L. \tag{31}$$

Therefore, the divergence rate of $\left|\mu_3^{(k)}\right|$ is exponential, and the slope of the linear equation that approximates the divergence is $3L$.

Analogous evaluations are performed for $\mu_{n-1}^{(k+1)}$ (9):

$$\mu_{n-1}^{(k+1)} = a\mu_{n-1}^{(k)} - a\left(\mu_1^{(k)}\mu_{n-2}^{(k)} + \mu_2^{(k)}\mu_{n-3}^{(k)} + \ldots + \mu_{n-2}^{(k)}\mu_1^{(k)}\right); \quad k = 0,1,2,\ldots. \tag{32}$$

Let us introduce the following auxiliary maps:

$$\begin{aligned} &\beta_{n-1}^{(k+1)} = a\beta_{n-1}^{(k)}\left(1-2\lambda_0^{(k)}\right);\\ &\eta_{1,n-2}^{(k+1)} = a\mu_1^{(k)}\mu_{n-2}^{(k)}; \quad \eta_{2,n-3}^{(k+1)} = a\mu_2^{(k)}\mu_{n-3}^{(k)}; \quad \ldots; \quad \eta_{n-2,1}^{(k+1)} = a\mu_{n-2}^{(k)}\mu_1^{(k)}; \end{aligned} \tag{33}$$

where $k = 0,1,2,\ldots$.

The divergence rate of $\ln\left|\beta_{n-1}^{(k)}\right|$ is equal to L. But

$$\lim_{k\to\infty}\frac{1}{k}\ln\left|\eta_{1,n-2}^{(k)}\right| = \lim_{k\to\infty}\frac{1}{k}\ln\left|\eta_{2,n-3}^{(k)}\right| = \ldots = \lim_{k\to\infty}\frac{1}{k}\ln\left|\eta_{n-2,1}^{(k)}\right| = (n-1)L. \tag{34}$$

Therefore, the divergence rate of $\left|\mu_{n-1}^{(k)}\right|$ is exponential and the slope of the linear equation that approximates the divergence is $(n-1)L$. The auxiliary parameter $\left|\mu_{n-1}^{(k)}\right|$ is of order $n-1$. Therefore, the divergence rate of this auxiliary parameter is equal to $(n-1)L$.

5. Computational Experiments

5.1. The Iterative Map of the Recurrent Eigenvalue in the Fractional Difference Logistic Map of Nilpotent Matrices

Let us consider the Caputo fractional difference logistic map of nilpotent matrices of order $n = 6$ and fractional order $\nu = 0.8$ (Equation (13)). Note that such a map is governed by n scalar maps (Equation (14))—a scalar fractional difference logistic map of a recurrent eigenvalue $\lambda_0^{(k)}$ (which coincides with Equation (10)) and intertwined maps of auxiliary parameters $\mu_1^{(k)}, \mu_2^{(k)}, \ldots, \mu_5^{(k)}$.

The bifurcation diagram of the recurrent eigenvalue $\lambda_0^{(k)}$ is plotted in the top panel of Figure 1 ($\lambda_0^{(0)} = 0.1$; 500 iterations are omitted for the transients). Vertical red dashed lines indicate the parameter value a selected for subsequent analysis of the fractional difference logistic map of the following nilpotent matrices: $a = 1.2$ (Section 5.3.2), $a = 3.35$ (Section 5.3.3), $a = 3.36$ (Section 5.3.4), $a = 3.378$ (Section 5.3.4), and $a = 3.67$ (Section 5.2). The Lyapunov exponent of $\lambda_0^{(k)}$ is shown in the bottom panel of Figure 1 (positive values are depicted in red).

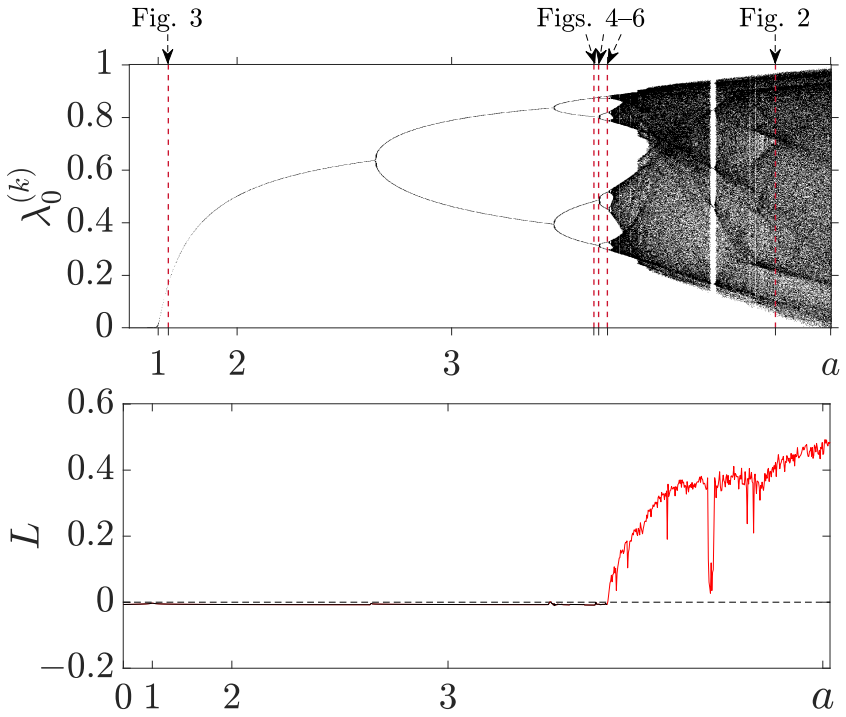

Figure 1. The bifurcation diagram of the recurrent eigenvalue $\lambda_0^{(k)}$ is shown in the **top panel** ($\nu = 0.8$; $\lambda_0^{(0)} = 0.1$; 500 iterations are omitted for the transients). Vertical red dashed lines denote the values of parameter a (a is set to 1.2, 3.35, 3.36, 3.378, and 3.67) used to explore different types of dynamical behavior investigated in Sections 5.3.2–5.3.4 and Section 5.2, respectively. The Lyapunov exponent L computed for the fractional difference logistic map is depicted in the **bottom panel** (values greater than zero are marked in red).

5.2. The Divergence of the Fractional Difference Logistic Map of Nilpotent Matrices

Let us proceed with the most counterintuitive dynamics of the fractional difference logistic map of nilpotent matrices—specifically, the divergence that may occur even when a recurrent eigenvalue remains bounded [41]. When the matrix order exceeds 2, distinct rates of divergence are observed.

The rates of divergence of the fractional difference logistic map of nilpotent matrices of order 6 are shown in Figure 2. The parameter a is set to 3.67 and the order of the fractional difference ν is equal to 0.8; $\lambda_0^{(0)} = 0.1$. Lyapunov exponent L of the fractional scalar logistic

map at $a = 3.67$ is 0.3808. The growth of $\ln\left|\mu_1^{(k)}\right|$ is approximated by the black dashed line with the slope equal to $0.3861 \approx L$. The growth of $\ln\left|\mu_2^{(k)}\right|$ is approximated by the blue dashed line with the slope equal to $0.7737 \approx 2L$. The growth of $\ln\left|\mu_3^{(k)}\right|$ is approximated by the green dashed line with the slope equal to $1.1594 \approx 3L$. The growth of $\ln\left|\mu_4^{(k)}\right|$ is approximated by the red dashed line with the slope equal to $1.5443 \approx 4L$. The growth of $\ln\left|\mu_5^{(k)}\right|$ is approximated by the orange dashed line with the slope equal to $1.9323 \approx 5L$.

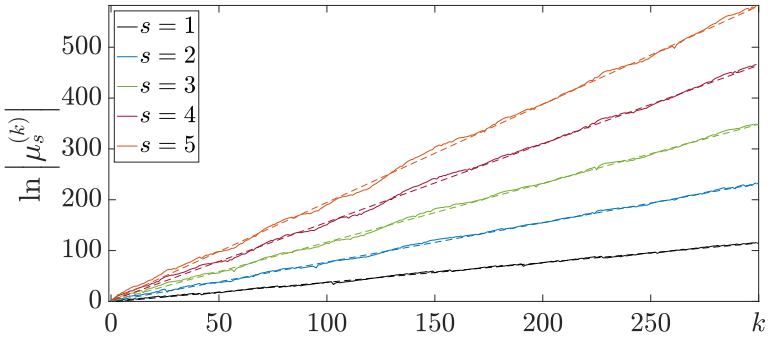

Figure 2. The divergence rate of the auxiliary parameters of the fractional difference logistic map of nilpotent matrices is exponential. The dynamics of $\ln\left|\mu_1^{(k)}\right|$, $\ln\left|\mu_2^{(k)}\right|$, $\ln\left|\mu_3^{(k)}\right|$, $\ln\left|\mu_4^{(k)}\right|$, and $\ln\left|\mu_5^{(k)}\right|$; $k = 0, 1, \ldots, 300$ is shown at $a = 3.67$ and $\nu = 0.8$. The dashed lines depict linear approximation of $\ln\left|\mu_s^{(k)}\right|$; $s = 1, \ldots, 5$. The growth rate of $\ln\left|\mu_s^{(k)}\right|$ is approximately equal to sL, where the Lyapunov exponent $L = 0.3808$.

5.3. The Convergence of the Fractional Difference Logistic Map of Nilpotent Matrices

5.3.1. The Algorithm Used to Identify the Type of Convergence

The type of convergence (exponential or power law) is identified by means of the algorithm comprising the following steps. Firstly, the analyzed time series is plotted on log–linear and log–log scales. Then, a linear (first degree polynomial) approximation is constructed for log–linear and log–log scales. Finally, the approximation error (the normalized root mean square error) is computed on log–linear and log–log scales.

Ideally, the approximation error for exponential convergence should be zero on the log–linear scale, and the approximation error for power law convergence should be zero on the log–log scale. This can be explained by the following elementary formulas. An exponential function $y_1 = e^{ax}$ becomes a linear function on the log–linear scale: $y_1 = \ln\left(e^{ax}\right) = ax$. A power law function $y_2 = x^b$ becomes a linear function on the log–log scale: $\ln\left(y_2\right) = \ln\left(x^b\right) = b\ln\left(x\right)$.

In reality, the trajectories captured by numerical simulation algorithms are contaminated by noise. Moreover, one may not expect that the convergence of a complex fractional difference logistic map of nilpotent matrices should be strictly exponential or strictly governed by the power law. Therefore, the classification algorithm (between exponential and power law convergence) is based on the comparison of the approximation errors of the same time series in the log–linear and log–log scales. The residuals of the approximation errors in the log–log scale will be denoted as R_p and the linear–log scale—as R_e.

5.3.2. Monotonous Convergence of the Fractional Difference Logistic Map of Nilpotent Matrices at $a = 1.2$

The monotonous convergence of the fractional difference logistic map of nilpotent matrices of order 6 to a stable period-1 regime is investigated in Figure 3 ($a = 1.2$; $\nu = 0.8$; $\lambda_0^{(0)} = 0.1$).

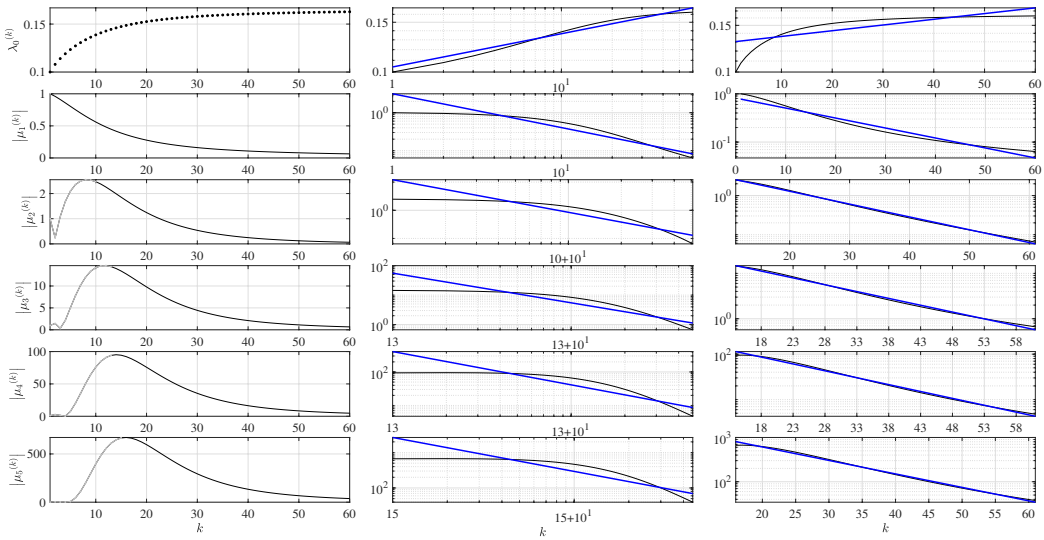

Figure 3. Monotonous convergence of the fractional difference logistic map of nilpotent matrices at $a = 1.2$, $\nu = 0.8$ and $\lambda_0^{(0)} = 0.1$. Only the regions of convergence of $\left|\mu_s^{(k)}\right|; s = 1, \ldots, 5$ (marked in black solid lines in **the left column**) are plotted on the log–log scale (**the middle column**) and the log–linear scale (**the right column**).

The left column of Figure 3 represents the evolution of the recurrent eigenvalue $\lambda_0^{(k)}$ and the modulus of the auxiliary parameters $\left|\mu_s^{(k)}\right|; s = 1, \ldots, 5$ on the linear scale. The middle column shows the evolution of $\lambda_0^{(k)}$ and $\left|\mu_s^{(k)}\right|; s = 1, \ldots, 5$ on the log–log scale. Analogously, the right column shows the evolution of $\lambda_0^{(k)}$ and $\left|\mu_s^{(k)}\right|; s = 1, \ldots, 5$ on the log–linear scale.

It is interesting to observe that the convergence of $\lambda_0^{(k)}$ occurs according to the power law: $R_p = 0.0217 < R_e = 0.0570$ (Table 1). This fact is supported by the results reported in [27] and coincides with the rigorous theoretical proof published in [34]: the convergence of the scalar fractional difference logistic map to a stable fixed point follows the power law.

The dynamics of the auxiliary parameters $\left|\mu_s^{(k)}\right|; s = 1, \ldots, 5$ is intertwined with the dynamics of the recurrent eigenvalue $\lambda_0^{(k)}$ (Equation (14)). The auxiliary parameter $\left|\mu_1^{(k)}\right|$ monotonously converges to the quiet state: $\lim_{k \to \infty} \left|\mu_1^{(k)}\right| = 0$. However, higher-order auxiliary parameters experience a finite-time blow-up before settling into a monotonous convergence to the quiet state (Figure 3). The higher the order of the auxiliary parameter $\mu_s^{(k)}$, the larger the finite time blow-up: $\left|\mu_2^{(k)}\right|$ reaches 2.472 at $k = 10$, but $\left|\mu_5^{(k)}\right|$ reaches 665.5 at $k = 15$ (Figure 3). Only the converging parts of $\left|\mu_s^{(k)}\right|; s = 1, \ldots, 5$ (marked in black solid lines in the left column) are further investigated on the log–log and log–linear scales in Figure 3.

The convergence of the auxiliary parameters occurs according to the exponential law (Figure 3, Table 1). One can observe the encounter of two different phenomena: the power law convergence of the scalar fractional difference logistic map and the exponential convergence induced by the nilpotent matrices. The "traces" of the power law convergence of $\lambda_0^{(k)}$ are still observable on the log–linear scale of $\left|\mu_1^{(k)}\right|$: the graph of $\left|\mu_1^{(k)}\right|$ does not coincide with the approximating line of linear regression. In general, such an effect tends to vanish for higher-order auxiliary parameters and can be quantified by the ratio between R_p and R_e. In this particular case, $\frac{R_p}{R_e} = 4.466$ for $\left|\mu_1^{(k)}\right|$, but $\frac{R_p}{R_e} = 34.944$ for $\left|\mu_2^{(k)}\right|$ (Figure 3, Table 1).

Table 1. The residuals of approximation R_p and R_e computed for auxiliary parameters $\left|\mu_s^{(k)}\right|$, $s = 1, \ldots, 5$ for the set of parameters used in Figures 3–6.

Parameter Set	Aux. Param.	R_p	R_e	R_p/R_e
$a = 1.2$, $\lambda_0^{(0)} = 0.1$ (Figure 3)	λ_0	2.17×10^{-2}	5.70×10^{-2}	<1
	μ_1	1.10×10^{0}	2.47×10^{-1}	>1
	μ_2	2.14×10^{0}	6.11×10^{-2}	>1
	μ_3	1.43×10^{0}	6.81×10^{-2}	>1
	μ_4	1.45×10^{0}	1.19×10^{-1}	>1
	μ_5	1.30×10^{0}	1.16×10^{-1}	>1
$a = 3.35$, $\lambda_0^{(0)} = 0.3$ (Figure 4)	μ_1	2.94×10^{0}	4.63×10^{0}	<1
	μ_2	2.34×10^{1}	4.91×10^{0}	>1
	μ_3	1.65×10^{1}	3.03×10^{0}	>1
	μ_4	1.60×10^{1}	3.07×10^{0}	>1
	μ_5	1.10×10^{1}	2.65×10^{0}	>1
$a = 3.36$, $\lambda_0^{(0)} = 0.12$ (Figure 5)	μ_1	8.78×10^{1}	1.29×10^{0}	>1
	μ_2	8.48×10^{1}	1.33×10^{0}	>1
	μ_3	2.87×10^{2}	1.50×10^{0}	>1
	μ_4	1.94×10^{3}	1.78×10^{0}	>1
	μ_5	7.63×10^{2}	1.64×10^{0}	>1
$a = 3.378$, $\lambda_0^{(0)} = 0.078$ (Figure 6)	μ_1	1.14×10^{2}	1.56×10^{0}	>1
	μ_2	4.54×10^{3}	1.79×10^{0}	>1
	μ_3	2.67×10^{3}	1.77×10^{0}	>1
	μ_4	5.28×10^{3}	1.91×10^{0}	>1
	μ_5	8.64×10^{2}	1.74×10^{0}	>1

5.3.3. Convergence After the Finite-Time Divergence at $a = 3.35$

The convergence of the auxiliary parameters $\left|\mu_s^{(k)}\right|$; $s = 1, \ldots, 5$ (after finite-time divergence) is depicted in Figure 4 ($a = 3.35$; $\nu = 0.8$; $\lambda_0^{(0)} = 0.3$). The effect of finite-time divergence in iterative maps of nilpotent matrices occurs when the chaotic system approaches the onset of chaos (the auxiliary parameters blow-up to large but finite values and then converge to the quiet state) [35,39]. Only the converging parts (plotted in dark solid lines) of $\left|\mu_s^{(k)}\right|$; $s = 1, \ldots, 5$ are investigated in Figure 4.

It is interesting to observe that the convergence of $\left|\mu_1^{(k)}\right|$ still occurs according to the power law as $R_p < R_e$ (Table 1). However, the convergence of all other auxiliary parameters with higher indexes is exponential (Figure 4; Table 1). The exponential effects induced by the nilpotent matrices suppress the power law convergence effects induced by the scalar chaotic map.

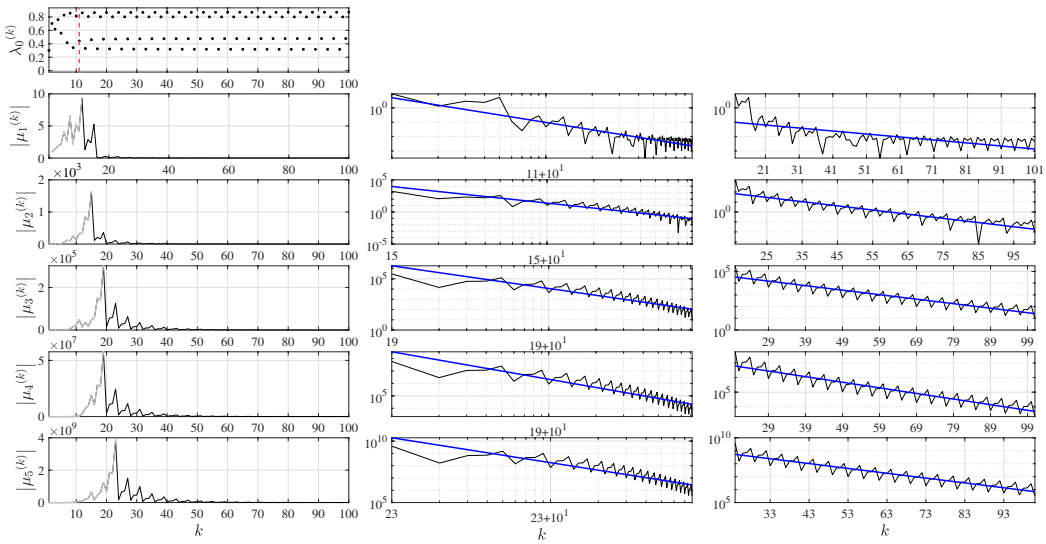

Figure 4. Convergence after the finite-time divergence of the fractional difference logistic map of nilpotent matrices at $a = 3.35$ and $\nu = 0.8$ ($\lambda_0^{(0)} = 0.3$). Only the converging parts of $\left|\mu_s^{(k)}\right|; s = 1, \ldots, 5$ (marked in black solid lines in **the left column**) are plotted on the log–log scale (**the middle column**) and the log–linear scale (**the right column**). The vertical red dashed line in the upper-left panel represents the largest peak of $\left|\mu_1^{(k)}\right|$ what corresponds to the period-doubling bifurcation of $\lambda_0^{(0)}$.

5.3.4. Convergence After the Intermittent Bursting at $a = 3.36$ and $a = 3.378$

It is well known that nilpotent matrices may induce such effects as finite-time divergence (when the system is approaching the onset of chaos) and explosive divergence (when the Lyapunov coefficient is positive and the system is in the state of fully developed chaos) in nonfractional maps of matrices [35,39]. However, a completely different effect (characterized as intermittent bursting [41]) can be observed in the discrete fractional difference logistic map of nilpotent matrices. Each burst occurs after the period-doubling bifurcation of the recurrent eigenvalue $\lambda_0^{(k)}$ [41].

The effect of intermittent bursting is illustrated in Figure 5 ($a = 3.36$; $\nu = 0.8$; $\lambda_0^{(0)} = 0.12$). As previously mentioned, only the converging parts of $\left|\mu_s^{(k)}\right|; s = 1, \ldots, 5$ (plotted in solid black lines) are tested for the convergence rates. It can be seen that the rate of convergence is exponential (Figure 5; Table 1).

Computational experiments are continued by increasing the parameter a to 3.378 and moving even closer to the onset of chaos (Figure 6). Again, only the converging parts of $\left|\mu_s^{(k)}\right|; s = 1, \ldots, 5$ (plotted in solid black lines) are tested for the convergence rate, which is determined to be exponential (Figure 6; Table 1).

As already mentioned, intermittent bursting occurs after the period-doubling bifurcation of the recurrent eigenvalue. This effect is also illustrated for a transient trajectory of the fractional difference logistic map of nilpotent matrices, which represents a cascade of period-doubling bifurcations of the recurrent eigenvalue over time (Figure 7). Note that such trajectories, called cascade of bifurcation-type trajectories, for the scalar fractional difference logistic map have already been reported in [82].

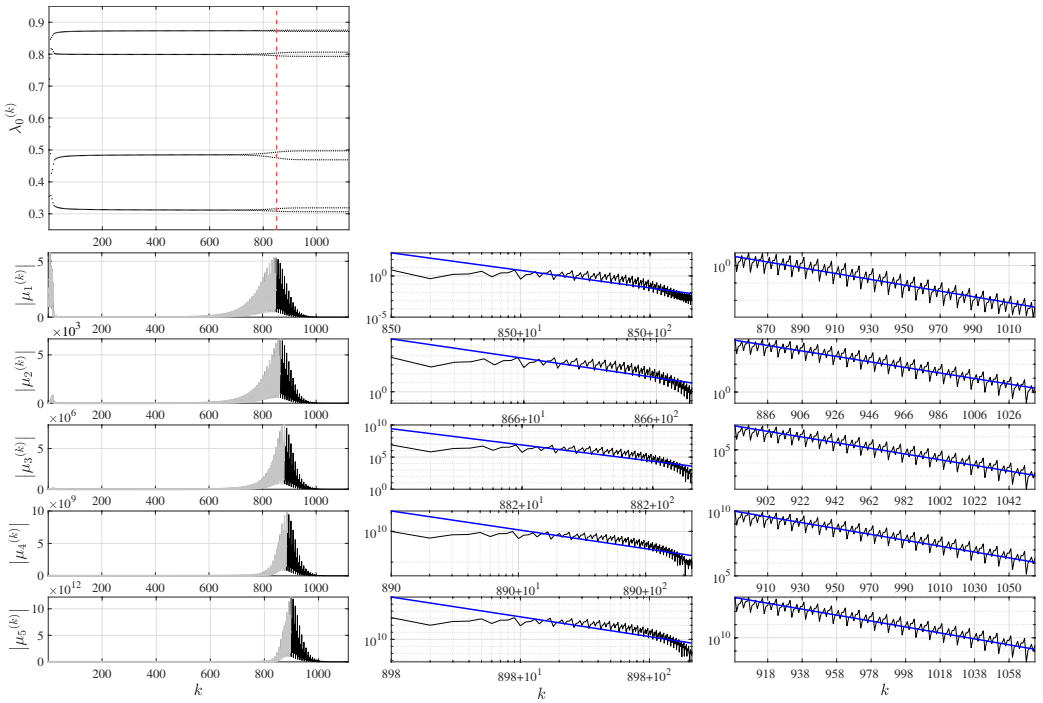

Figure 5. Convergence after the intermittent bursting of the fractional difference logistic map of nilpotent matrices at $a = 3.36$, $\nu = 0.8$ and $\lambda_0^{(0)} = 0.12$. Only the converging parts of $\left|\mu_s^{(k)}\right|$; $s = 1, \ldots, 5$ (marked in black solid lines in **the left column**) are plotted on the log–log scale (**the middle column**) and the log–linear scale (**the right column**). The vertical red dashed line in the upper-left panel represents the largest peak of $\left|\mu_1^{(k)}\right|$ after the initial finite-time divergence what corresponds to the period-doubling bifurcation of $\lambda_0^{(0)}$.

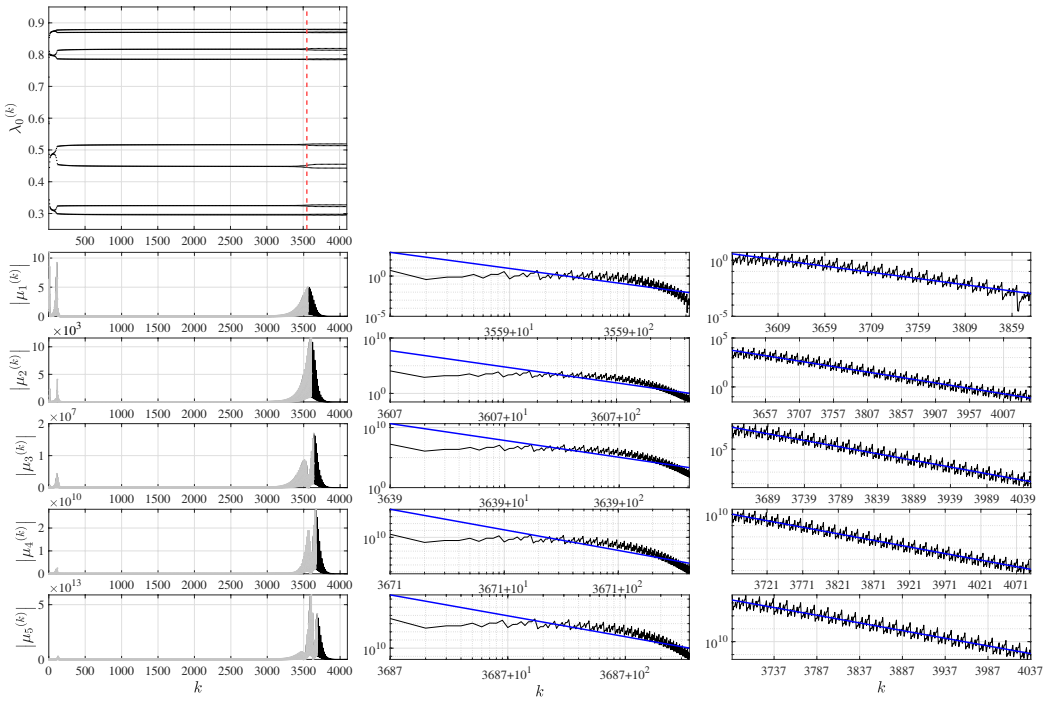

Figure 6. Convergence after the intermittent bursting of the fractional difference logistic map of nilpotent matrices at $a = 3.378$ and $\nu = 0.8$ ($\lambda_0^{(0)} = 0.078$). Only the converging parts of $\left|\mu_s^{(k)}\right|$; $s = 1, \ldots, 5$ (marked in black solid lines in **the left column**) are plotted on the log–log scale (**the middle column**) and the log–linear scale (**the right column**). The vertical red dashed line in the upper-left panel represents the largest peak of $\left|\mu_1^{(k)}\right|$ after the initial finite-time divergence what corresponds to the period-doubling bifurcation of $\lambda_0^{(0)}$.

https://doi.org/10.3390/fractalfract10010040

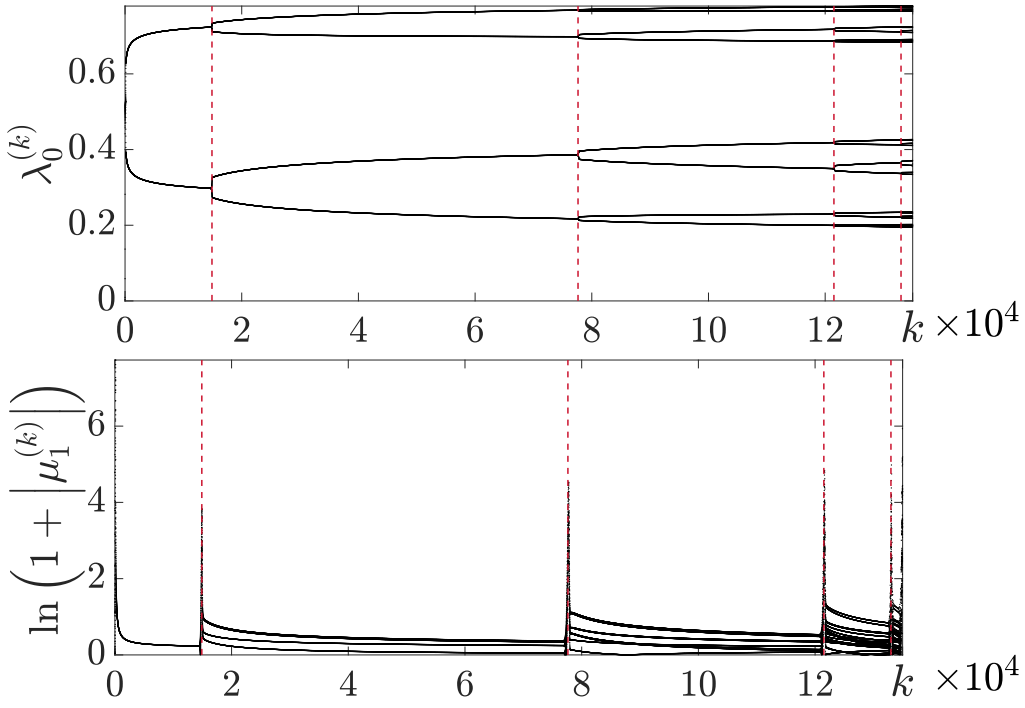

Figure 7. The fractional difference logistic map of nilpotent matrices of order 6. The burst peaks of $\ln\left(1+\left|\mu_1^{(k)}\right|\right)$ in the fractional logistic map of matrices appear at the same time instants as the period doubling of $\lambda_0^{(k)}$ is observed at k equal to 14,900, 77,640, 121,500, and 133,000. The parameters of Caputo fractional difference logistic map is set to $a = 3.39$ and $\nu = 0.1$ ($\lambda_0^{(0)} = 0.001$). The total number of iterations performed is 135,000.

6. Discussion and Concluding Remarks

It is well-known that the divergence rate of the fractional difference logistic map from a fixed point can be exponential, but convergence to a fixed point occurs according to the power law [82]. This fact carries a number of implications for studying the complex behavior of fractional difference chaotic maps. For example, the computation of the Lyapunov exponent for the characterization of the convergence of the fractional difference logistic map is meaningless.

This fact can be represented by the following example. Let us assume that the initial perturbation δ_0 changes in time according to the exponential law: $|\delta(t)| = e^{\lambda t}|\delta_0|$. Then, the Lyapunov exponent reads [83] $\lim\limits_{t\to\infty}\lim\limits_{|\delta_0|\to 0}\frac{1}{t}\ln\frac{|\delta(t)|}{|\delta_0|} = \lambda$. Therefore, the Lyapunov exponent for periodic orbits of the standard scalar logistic map is negative, since convergence to such orbits almost everywhere occurs at an exponential rate [84].

Now, let us assume that the initial perturbation changes according to the power law: $|\delta(t)| = t^{\lambda}|\delta_0|$. Then, $\lim\limits_{t\to\infty}\lim\limits_{|\delta_0|\to 0}\frac{1}{t}\ln\frac{|\delta(t)|}{|\delta_0|} = \lambda\lim\limits_{t\to\infty}\frac{\ln t}{t} = 0$. This limits the applicability of classical algorithms based on the computation of Lyapunov exponents for the exploration of the convergence of fractional difference maps. In fact, it can be observed in Figure 1 that the reconstructed Lyapunov exponents for the scalar fractional difference logistic map of eigenvalues are equal to zero everywhere except in the region where the map exhibits chaotic behavior.

The logistic map (being paradigmatic models of chaotic systems) is widely exploited for the investigation of spatially extended systems. Coupled Map Lattices of the logistic maps (including fractional logistic maps) remain an active area of research. Spatiotemporal

synchronization, traveling waves, and coherent states—these are just a few of the many effects observed in the dynamics of chaotic Coupled Map Lattices [40,85–87].

The complexity of a system comprising fractional difference logistic maps can be increased not only by extending the number of coupled nodes in the spatial domain, but also by making each node more complex. The fractional difference logistic map of nilpotent matrices is exactly the case when the extension is performed at the node itself.

It appears that the dynamics of such a fractional system of nilpotent matrices becomes very complicated. The divergence of the system from a fixed point is governed by the exponential law. The divergence occurs when the Lyapunov exponent of the scalar fractional system is positive. The divergence rate of the auxiliary parameters is also exponential, but the rate is a multiple of the Lyapunov exponent of the scalar system. Moreover, the exponential divergence rate of the auxiliary parameters depends on their order, with the divergence rate being equal to the order multiplied by the Lyapunov exponent of the scalar map. This explains the structural role of nilpotency in amplifying exponential effects.

However, the situation becomes much more tortuous with the convergence of the fractional system of nilpotent matrices to the fixed point. The convergence of the system is governed by the interplay of two different phenomena: the power law governing the convergence of the scalar fractional system and the exponential convergence induced by nilpotent matrices.

Such an interplay opens ample opportunities for designing Coupled Map Lattices of fractional logistic maps of nilpotent matrices. For example, an encoding scheme for multiple digital images in a single Coupled Map Lattice of classical logistic maps of nilpotent matrices is proposed in [40]. Extending such an encoding scheme to its fractional counterpart would open new possibilities to extend the carrying capacity of the scheme and enhance the security of the encoding algorithm. The transient divergence induced by the competition between the power law and exponential mechanisms at each node of such lattices poses significant challenges for spatiotemporal synchronization and control of transient processes. At the same time, these challenges may be viewed as advantages in terms of the security of the encoding scheme. The development of such schemes based on complex convergence patterns remains the definite objective of future research.

The present analysis is restricted to the Caputo fractional difference logistic map of nilpotent matrices. In particular, the scalar non-fractional logistic map is a one-dimensional non-invertible iterative map. Extending the present analysis to more complex classes of iterative systems, such as two-dimensional maps (for example, the Rulkov neuron map) or fully invertible maps (for example, the bouncing ball problem), represents a natural and promising direction for future research. These extensions may reveal additional dynamical features and broaden the proposed analytical framework.

Author Contributions: Conceptualization, R.S., M.E. and M.R.; methodology, R.S., M.E. and M.R.; software, R.S. and A.K.; validation, M.E. and M.R.; formal analysis, R.S., A.K. and M.R.; investigation, A.K.; resources, A.K.; data curation, R.S. and A.K.; writing—original draft preparation, R.S., A.K., M.E. and M.R.; writing—review and editing, R.S., A.K., M.E. and M.R.; visualization, R.S. and A.K.; supervision, M.E. and M.R.; project administration, R.S. and M.R.; funding acquisition, R.S., M.E. and M.R. All authors have read and agreed to the published version of the manuscript.

Funding: This research is funded by the Research Council of Lithuania (LMTLT), Project No. S-MIP-25-52 (Finite-time divergence in differential equations of nilpotent matrices—theory and applications (DENM)).

Data Availability Statement: The datasets generated during and/or analyzed during the current study are available from the corresponding author on reasonable request.

Conflicts of Interest: The authors declare no conflicts of interest.

References

1. Lorenz, E.N. The problem of deducing the climate from the governing equations. *Tellus* **1964**, *16*, 1–11. [CrossRef]
2. May, R. Simple mathematical models with very complicated dynamics. *Nature* **1976**, *261*, 459–467. [CrossRef] [PubMed]
3. Feigenbaum, M.J. Quantitative universality for a class of nonlinear transformations. *J. Stat. Phys.* **1978**, *19*, 25–52. [CrossRef]
4. Cvitanović, P. Universality in chaos. In *Universality in Chaos*, 2nd ed.; Routledge: New York, NY, USA, 2017; pp. 2–32. [CrossRef]
5. Strogatz, S.H. *Nonlinear Dynamics and Chaos: With Applications to Physics, Biology, Chemistry, and Engineering*, 2nd ed.; CRC Press: Boca Raton, FL, USA, 2001. [CrossRef]
6. Barreira, L. *Lyapunov Exponents*; Springer: Berlin/Heidelberg, Germany, 2017; Volume 1002. [CrossRef]
7. Ausloos, M. *The Logistic Map and the Route to Chaos: From the Beginnings to Modern Applications*; Springer Science & Business Media: New York, NY, USA, 2006. [CrossRef]
8. Bland, M. *An Introduction to Medical Statistics*; Oxford University Press: New York, NY, USA, 2015.
9. Abdellah, M. Generalized logistic map and its applications. *AIP Adv.* **2025**, *15*, 035239. [CrossRef]
10. Dubois, D.M. Mathematical foundations of discrete and functional systems with strong and weak anticipations. In *Anticipatory Behavior in Adaptive Learning Systems*; Lecture Notes in Computer Science; Springer: Berlin/Heidelberg, Germany, 2003; pp. 110–132. [CrossRef]
11. Leydesdorff, L.; Franse, S. The communication of meaning in social systems. *Syst. Res. Behav. Sci.* **2009**, *26*, 109–117. [CrossRef]
12. Alexandrov, V.; Gajdusek, M.F.; Knight, C.G.; Yotova, A. *Global Environmental Change: Challenges to Science and Society in Southeastern Europe*; Springer: Berlin/Heidelberg, Germany, 2010. [CrossRef]
13. Miśkiewicz, J.; Ausloos, M. A logistic map approach to economic cycles. (I). The best adapted companies. *Phys. A Stat. Mech. Appl.* **2004**, *336*, 206–214. [CrossRef]
14. Ausloos, M.; Clippe, P.; Miśkiewicz, J.; Pe¸kalski, A. A (reactive) lattice-gas approach to economic cycles. *Phys. A Stat. Mech. Appl.* **2004**, *344*, 1–7. [CrossRef]
15. Miśkiewicz, J.; Ausloos, M. Delayed information flow effect in economy systems. An ACP model study. *Phys. A Stat. Mech. Appl.* **2007**, *382*, 179–186. [CrossRef]
16. Edelman, M. Evolution of Systems with Power-Law Memory: Do We Have to Die? (Dedicated to the Memory of Valentin Afraimovich). In *Demography of Population Health, Aging and Health Expenditures*; Skiadas, C.H., Skiadas, C., Eds.; Springer International Publishing: Cham, Switzerland, 2020; pp. 65–85. [CrossRef]
17. Tarasov, V.E.; Tarasova, V.V. *Economic Dynamics with Memory: Fractional Calculus Approach*; Walter de Gruyter: Berlin/Heidelberg, Germany; Boston, MA, USA, 2021. [CrossRef]
18. Petráš, I. Fractional-order control: New control techniques. In *Fractional Order Systems*; Radwan, A.G., Khanday, F.A., Said, L.A., Eds.; Emerging Methodologies and Applications in Modelling; Academic Press: London, UK, 2022; pp. 71–106. [CrossRef]
19. Reed, E.A.; Ramos, G.; Bogdan, P.; Pequito, S. The role of long-term power-law memory in controlling large-scale dynamical networks. *Sci. Rep.* **2023**, *13*, 19502. [CrossRef]
20. Cylke, A.; Banerjee, S. Gene expression cycles drive non-exponential bacterial growth. *Phys. Rev. Res.* **2025**, *7*, 033123. [CrossRef]
21. Ortigueira, M.D. Principles of fractional signal processing. *Digit. Signal Process.* **2024**, *149*, 104490. [CrossRef]
22. Yang, Q.; Chen, D.; Zhao, T.; Chen, Y. Fractional calculus in image processing: A review. *Fract. Calc. Appl. Anal.* **2016**, *19*, 1222–1249. [CrossRef]
23. Zhu, L.; Jiang, D.; Ni, J.; Wang, X.; Rong, X.; Ahmad, M.; Chen, Y. A stable meaningful image encryption scheme using the newly-designed 2D discrete fractional-order chaotic map and Bayesian compressive sensing. *Signal Process.* **2022**, *195*, 108489. [CrossRef]
24. Edelman, M. On the fractional Eulerian numbers and equivalence of maps with long term power-law memory (integral Volterra equations of the second kind) to Grünvald-Letnikov fractional difference (differential) equations. *Chaos* **2015**, *25*, 073103. [CrossRef]
25. Edelman, M. Cycles in asymptotically stable and chaotic fractional maps. *Nonlinear Dyn.* **2021**, *104*, 2829–2841. [CrossRef]
26. Tarasov, V.E. Multi-kernel discrete maps with memory from general fractional differential and integral equations. *Nonlinear Dyn.* **2025**, *113*, 34341–34369. [CrossRef]
27. Edelman, M. Fractional Maps and Fractional Attractors. Part II: Fractional Difference Caputo α-Families of Maps. *Interdiscip. J. Discontin. Nonlinearity Complex.* **2015**, *4*, 391–402. [CrossRef]
28. Jonnalagadda, J. Periodic solutions of fractional nabla difference equations. *Commun. Appl. Anal.* **2016**, *20*, 585–610.
29. Jonnalagadda, J.M. Quasi-periodic solutions of fractional nabla difference systems. *Fract. Differ. Calc.* **2017**, *7*, 339–355. [CrossRef]
30. Kaslik, E.; Sivasundaram, S. Non-existence of periodic solutions in fractional-order dynamical systems and a remarkable difference between integer and fractional-order derivatives of periodic functions. *Anal. Real World Appl.* **2012**, *13*, 1489–1497. [CrossRef]
31. Edelman, M. Asymptotically periodic and bifurcation points in fractional difference maps. *Fractal Fract.* **2025**, *9*, 231. [CrossRef]

32. Edelman, M.; Helman, A.B.; Smidtaite, R. Bifurcations and transition to chaos in generalized fractional maps of the orders $0 < \alpha < 1$. *Chaos* **2023**, *33*, 063123. [CrossRef]
33. Edelman, M.; Tarasov, V.E. Fractional standard map. *Phys. Lett. A* **2009**, *374*, 279–285. [CrossRef]
34. Anh, P.T.; Babiarz, A.; Czornik, A.; Niezabitowski, M.; Siegmund, S. Asymptotic properties of discrete linear fractional equations. *Bull. Pol. Acad. Sci.* **2019**, *67*, 749–759. [CrossRef]
35. Navickas, Z.; Smidtaite, R.; Vainoras, A.; Ragulskis, M. The logistic map of matrices. *Discret. Contin. Dyn. Syst. Ser. B* **2011**, *16*, 927–944. [CrossRef]
36. Kaneko, K. Coupled map lattice. In *Chaos, Order, and Patterns*; Springer: Berlin/Heidelberg, Germany, 1991; pp. 237–247.
37. Gang, H.; Zhilin, Q. Controlling spatiotemporal chaos in coupled map lattice systems. *Phys. Rev. Lett.* **1994**, *72*, 68–71. [CrossRef]
38. Hagerstrom, A.M.; Murphy, T.E.; Roy, R.; Hövel, P.; Omelchenko, I.; Schöll, E. Experimental observation of chimeras in coupled-map lattices. *Nat. Phys.* **2012**, *8*, 658–661. [CrossRef]
39. Smidtaite, R.; Navickas, Z.; Ragulskis, M. Clocking divergence of iterative maps of matrices. *Commun. Nonlinear Sci. Numer. Simul.* **2021**, *95*, 105589. [CrossRef]
40. Smidtaite, R.; Ragulskiene, J.; Bikulciene, L.; Ragulskis, M. Hyper Coupled Map Lattices for Hiding Multiple Images. *Complexity* **2023**, *2023*, 8831078. [CrossRef]
41. Petkevičiūtė-Gerlach, D.; Šmidtaitė, R.; Ragulskis, M. Intermittent Bursting in the Fractional Difference Logistic Map of Matrices. *Int. J. Bifurc. Chaos* **2022**, *32*, 2230002. [CrossRef]
42. Bick, C.; Timme, M.; Kolodziejski, C. Adapting Predictive Feedback Chaos Control for Optimal Convergence Speed. *SIAM J. Appl. Dyn. Syst.* **2012**, *11*, 1310–1324. [CrossRef]
43. Yang, X.S.; He, X. Bat algorithm: Literature review and applications. *Int. J. Bio-Inspir. Com.* **2013**, *5*, 141–149. [CrossRef]
44. Davis, D.; Yin, W. Convergence rate analysis of several splitting schemes. In *Splitting Methods in Communication, Imaging, Science, and Engineering*; Springer: Berlin/Heidelberg, Germany, 2017; pp. 115–163. [CrossRef]
45. Huang, M.; Luo, R.; Fu, J.; Su, H. Robust exponential synchronization of a class of chaotic systems with variable convergence rates via the saturation control. *Complexity* **2020**, *2020*, 8293190. [CrossRef]
46. Wang, X.; Cao, J.; Yang, B.; Chen, F. Fast fixed-time synchronization control analysis for a class of coupled delayed Cohen-Grossberg neural networks. *J. Frankl. Inst.* **2022**, *359*, 1612–1639. [CrossRef]
47. Su, H.; Luo, R.; Huang, M.; Fu, J. Fast convergence control of a class of uncertain chaotic systems with input nonlinearity by using a new sliding mode controller. *Eur. J. Control* **2023**, *69*, 100751. [CrossRef]
48. Borowski, H.; Marden, J.R. Fast convergence in semianonymous potential games. *IEEE Trans. Control Netw. Syst.* **2015**, *4*, 246–258. [CrossRef]
49. Smith, L.N.; Topin, N. Super-convergence: Very fast training of neural networks using large learning rates. In *Proceedings of the Artificial Intelligence and Machine Learning for Multi-Domain Operations Applications, Baltimore, MD, USA, 14–18 April 2019*; SPIE: Bellingham, WA, USA, 2019; Volume 11006, pp. 369–386. [CrossRef]
50. Nguyen, H.T.; Al-Sumaiti, A.S.; Vu, V.P.; Al-Durra, A.; Do, T.D. Optimal power tracking of PMSG based wind energy conversion systems by constrained direct control with fast convergence rates. *Int. J. Electr. Power Energy Syst.* **2020**, *118*, 105807. [CrossRef]
51. Zhang, Z.; Chow, M.Y. Convergence analysis of the incremental cost consensus algorithm under different communication network topologies in a smart grid. *IEEE Trans. Power Syst.* **2012**, *27*, 1761–1768. [CrossRef]
52. Mohamed, E.A.; Ahmed, E.M.; Elmelegi, A.; Aly, M.; Elbaksawi, O.; Mohamed, A.A.A. An Optimized Hybrid Fractional Order Controller for Frequency Regulation in Multi-Area Power Systems. *IEEE Access* **2020**, *8*, 213899–213915. [CrossRef]
53. Zhang, H.; Liang, S.; Liang, J.; Han, Y. Convergence analysis of a distributed gradient algorithm for economic dispatch in smart grids. *Int. J. Elec. Power Energy Syst.* **2022**, *134*, 107373. [CrossRef]
54. Sun, Y.; Li, W.; Zhao, D. Convergence time and speed of multi-agent systems in noisy environments. *Chaos* **2012**, *22*, 043126. [CrossRef]
55. Cheng, L.; Wang, Y.; Ren, W.; Hou, Z.G.; Tan, M. On convergence rate of leader-following consensus of linear multi-agent systems with communication noises. *IEEE Trans. Autom.* **2016**, *61*, 3586–3592. [CrossRef]
56. Ma, Q.; Xu, X.; Zhang, R.; Xiong, Q.; Zhang, X.; Zhang, X. Robust consensus control of nonlinear multi-agent systems based on convergence rate estimation. *Int. J. Robust Nonlin.* **2023**, *33*, 2003–2021. [CrossRef]
57. Talaat, F.M.; Aljadani, A. AI-driven churn prediction in subscription services: Addressing economic metrics, data transparency, and customer interdependence. *Neural Comput. Appl.* **2025**, *37*, 8651–8676. [CrossRef]
58. Nobis, G.; Springenberg, M.; Aversa, M.; Detzel, M.; Daems, R.; Murray-Smith, R.; Nakajima, S.; Lapuschkin, S.; Ermon, S.; Birdal, T.; et al. Generative fractional diffusion models. *Adv. Neural Inf. Process. Syst.* **2024**, *37*, 25469–25509.
59. Nedić, A. Convergence rate of distributed averaging dynamics and optimization in networks. *Found. Trends Syst. Control.* **2015**, *2*, 1–100. [CrossRef]
60. Tarasov, V.E. Review of some promising fractional physical models. *Int. J. Mod. Phys. B* **2013**, *27*, 1330005. [CrossRef]
61. Uchaikin, V.V. *Fractional Derivatives for Physicists and Engineers*; Springer: Berlin/Heidelberg, Germany, 2013; Volume 2. [CrossRef]

62. Lu, L.; Yu, X. The fractional dynamics of quantum systems. *Ann. Phys.* **2018**, *392*, 260–271. [CrossRef]
63. Rihan, F.A. Numerical Modeling of Fractional-Order Biological Systems. *Abstr. Appl. Anal.* **2013**, *2013*, 816803. [CrossRef]
64. Chakraverty, S.; Jena, R.M.; Jena, S.K. *Time-Fractional Order Biological Systems with Uncertain Parameters*; Synthesis Lectures on Mathematics & Statistics Series; Springer: Cham, Switzerland, 2020. [CrossRef]
65. D'Alessandro, M.; Van Mieghem, P. Fractional derivative in continuous-time Markov processes and applications to epidemics in networks. *Phys. Rev. Res.* **2025**, *7*, 013017. [CrossRef]
66. Tenreiro Machado, J.A.; Silva, M.F.; Barbosa, R.S.; Jesus, I.S.; Reis, C.M.; Marcos, M.G.; Galhano, A.F. Some Applications of Fractional Calculus in Engineering. *Math. Probl. Eng.* **2010**, *2010*, 639801. [CrossRef]
67. Chen, W.; Sun, H.; Li, X. *Fractional Derivative Modeling in Mechanics and Engineering*; Springer: Berlin/Heidelberg, Germany, 2022. [CrossRef]
68. Arshad, M.; Lu, D.; Wang, J. (N+1)-dimensional fractional reduced differential transform method for fractional order partial differential equations. *Commun. Nonlinear Sci. Numer. Simul.* **2017**, *48*, 509–519. [CrossRef]
69. Fallahgoul, H.; Focardi, S.; Fabozzi, F. *Fractional Calculus and Fractional Processes with Applications to Financial Economics: Theory and Application*; Academic Press: New York, NY, USA, 2016.
70. Tarasov, V.E. Mathematical Economics: Application of Fractional Calculus. *Mathematics* **2020**, *8*, 660. [CrossRef]
71. Yousefpour, A.; Jahanshahi, H.; Munoz-Pacheco, J.M.; Bekiros, S.; Wei, Z. A fractional-order hyper-chaotic economic system with transient chaos. *Chaos Soliton. Fract.* **2020**, *130*, 109400. [CrossRef]
72. Tarasov, V.E. General Fractional Economic Dynamics with Memory. *Mathematics* **2024**, *12*, 2411. [CrossRef]
73. Zhang, X.; Feng, C.; Zhou, Y.; Deng, X. Finite-time tracking control for fractional-order nonlinear high-order parametric systems with time-varying control gain and external disturbances: An approximation-based adaptive control method. *Adv. Cont. Discr. Mod.* **2025**, *2025*, 144. [CrossRef]
74. Xu, X.; Lu, J.; Chen, J. Convergence Analysis of Iterative Learning Control for Initialized Fractional Order Systems. *Fractal Fract.* **2024**, *8*, 168. [CrossRef]
75. Louakar, A.; Vivek, D.; Kajouni, A.; Hilal, K. Iterative Learning Control for Hilfer-Type Fractional Stochastic Differential Systems: A Simulation Study for Robotic Applications. *Int. J. Robust Nonlin.* 2025, *early view*. [CrossRef]
76. Wang, J.; Fec, M.; Zhou, Y. Nonexistence of periodic solutions and asymptotically periodic solutions for fractional differential equations. *Commun. Nonlinear Sci. Numer. Simul.* **2013**, *18*, 246–256. [CrossRef]
77. Čermák, J.; Győri, I.; Nechvátal, L. On explicit stability conditions for a linear fractional difference system. *Fract. Calc. Appl. Anal.* **2015**, *18*, 651–672. [CrossRef]
78. Petkevičiūtė-Gerlach, D.; Timofejeva, I.; Ragulskis, M. Clocking convergence of the fractional difference logistic map. *Nonlinear Dyn.* **2020**, *100*, 3925–3935. [CrossRef]
79. Wang, Y.; Liu, S.; Li, H. On fractional difference logistic maps: Dynamic analysis and synchronous control. *Nonlin. Dyn.* **2020**, *102*, 579–588. [CrossRef]
80. Joshi, D.D.; Gade, P.M.; Bhalekar, S. Study of low-dimensional nonlinear fractional difference equations of complex order. *Chaos* **2022**, *32*, 113101. [CrossRef]
81. Hilborn, R.C. *Chaos and Nonlinear Dynamics: An Introduction for Scientists and Engineers*; Oxford University Press: New York, NY, USA, 2000. [CrossRef]
82. Edelman, M. Periodic Points, Stability, Bifurcations, and Transition to Chaos in Generalized Fractional Maps. *IFAC-PapersOnLine* **2024**, *58*, 131–142. [CrossRef]
83. Cencini, M.; Cecconi, F.; Vulpiani, A. *Chaos: From Simple Models to Complex Systems*; Series on advances in statistical mechanics; World Scientific: Singapore, 2010.
84. Pikovsky, A.; Politi, A. *Lyapunov Exponents: A Tool to Explore Complex Dynamics*; Cambridge University Press: Cambridge, UK, 2016.
85. Bukh, A.; Strelkova, G.; Anishchenko, V. Spiral wave patterns in a two-dimensional lattice of nonlocally coupled maps modeling neural activity. *Chaos Soliton. Fract.* **2019**, *120*, 75–82. [CrossRef]
86. Wan, W.; Harsh, R.; Meninno, A.; Dreher, P.; Sajan, S.; Guo, H.; Errea, I.; de Juan, F.; Ugeda, M.M. Evidence for ground state coherence in a two-dimensional Kondo lattice. *Nat. Commun.* **2023**, *14*, 7005. [CrossRef] [PubMed]
87. Ding, J.; Lei, Y.; Xie, J.; Small, M. Chaos synchronization of two coupled map lattice systems using safe reinforcement learning. *Chaos Soliton. Fract.* **2024**, *186*, 115241. [CrossRef]